

Properties of a liquid–gas interface at high-rate evaporation

S. I. Anisimov, D. O. Dunikov, V. V. Zhakhovskii, and S. P. Malysenko

Citation: *The Journal of Chemical Physics* **110**, 8722 (1999); doi: 10.1063/1.478779

View online: <http://dx.doi.org/10.1063/1.478779>

View Table of Contents: <http://scitation.aip.org/content/aip/journal/jcp/110/17?ver=pdfcov>

Published by the [AIP Publishing](#)

Articles you may be interested in

[Molecular dynamics study of nanoparticle stability at liquid interfaces: Effect of nanoparticle-solvent interaction and capillary waves](#)

J. Chem. Phys. **135**, 054704 (2011); 10.1063/1.3618553

[Boundary conditions at the vapor-liquid interface](#)

Phys. Fluids **23**, 030609 (2011); 10.1063/1.3567001

[Motion of a droplet near an evaporating liquid-gas interface](#)

Phys. Fluids **19**, 032101 (2007); 10.1063/1.2713098

[Boundary condition at a gas-liquid interphase](#)

AIP Conf. Proc. **585**, 583 (2001); 10.1063/1.1407612

[Thermocapillary interaction between a solid particle and a liquid-gas interface](#)

Phys. Fluids **9**, 2818 (1997); 10.1063/1.869394



Properties of a liquid–gas interface at high-rate evaporation

S. I. Anisimov, D. O. Dunikov,^{a)} V. V. Zhakhovskii, and S. P. Malyshenko^{a)}

Institute for High Temperatures, Russian Academy of Sciences, Izhorskaya 13/19, Moscow, 127412, Russia

(Received 24 August 1998; accepted 20 January 1999)

The effects of temperature and pressure nonuniformities at evaporation on the properties of liquid–gas interface are studied by molecular dynamics (MD) simulation and thermodynamic perturbation method on the basis of the van der Waals theory of capillarity. The structure and properties of the interfacial layer of equilibrium and nonequilibrium Lennard-Jones (12-6) systems are investigated. The surface tension, the two-particle distribution functions, the density fluctuation correlation lengths, and the evaporation coefficients are calculated using MD simulation. It is shown that the presence of the temperature gradient at the interface due to evaporation leads to reduction of the surface tension. The results of MD simulations are in agreement with the results of thermodynamic approach. © 1999 American Institute of Physics. [S0021-9606(99)50915-X]

I. INTRODUCTION

The problem of the influence of phase transitions on characteristics and properties of liquid–vapor interfaces has drawn serious attention for a long time. However, the known models of evaporation and condensation do not take into account actual structure and finite size of the interfacial layer that leads to essential restrictions. One of these restrictions is the ambiguity in definition of the surface temperature because of the presence of the temperature gradient in the interface. Commonly the interface is considered a dividing surface with zero thickness between two bulk phases with constant properties. There are some different choices of the dividing surface, which have different positions and properties. Usually as the dividing surface one uses the equimolar surface (the Gibbsian zero-adsorption dividing surface) or the surface of tension,¹ but there exist another way to define the dividing surface. In the equilibrium state there is no difference between temperatures of any dividing surfaces. In the nonequilibrium case, at evaporation or condensation the temperature gradient exists at the interface. The real interface has nonzero thickness, which in ordinary conditions is very narrow, e.g., about 1 nm for argon far from the critical point, but for high-rate phase transitions the temperature difference in the interfacial zone may cause a modification of the surface properties. Thus the noncorrect choice of the surface temperature cause errors in experimental definition of evaporation and condensation coefficients and the surface tension. Modification of the surface tension caused by the phase transition at the liquid–gas interface may lead to noticeable corrections in boundary conditions for hydrodynamic and heat and mass transfer problems. Besides, all published models are based on the assumption of the one-particle mechanism of evaporation and condensation; see for example, Refs. 2, 3. Recent computer simulations have shown that many body effects should be taken into account even for the simple liquids. The fluctuations of binding energy in the interfacial

zone⁴ and the molecular exchange at the surface⁵ were shown to play important role in the processes of evaporation and condensation.

Thus to describe the process of the intense phase transition we need an approach giving us a more complete description of the interface. In the present paper we used for this purpose an approach based on the modified van der Waals theory of capillarity and molecular dynamics simulations of the liquid–vapor interfaces.

II. THERMODYNAMICS

Within the van der Waals theory of capillarity the properties of a liquid–gas interface are determined by local density $\rho(\mathbf{r})$. The density at the interface varies continuously with position between two limit values in the bulk liquid and vapor. Thus the interface thickness may be determined as:

$$L = \Delta\rho \left(\frac{\partial\rho}{\partial z} \right)_e^{-1}, \quad (1)$$

where $\Delta\rho = \rho_l - \rho_g$ is the difference of densities of liquid and vapor, subscript l denotes properties of liquid and g denotes properties of gas, z is the coordinate normal to the surface, and $(\partial\rho/\partial z)_e$ is the density gradient at the Gibbsian zero-adsorption dividing surface (equimolar dividing surface). The surface tension is defined as a excess surface free energy:¹

$$\gamma = \int m[\rho(z)] \rho'(z)^2 dz \approx m \frac{(\Delta\rho)^2}{L}, \quad (2)$$

where $m[\rho(z)]$ is a parameter, which in the common case is a weak function of density. Equation (2) shows that any external influence, which can change the material distribution at the interface, should lead to a modification of the surface tension. It can be a pressure drop at the interface, e.g., the Laplacian pressure drop on the curved interface, or a temperature gradient due to phase transition, or nonuniformities of any other nature. This modification of the surface tension

^{a)}Authors to whom correspondence should be addressed; electronic mail: litp@dataforce.net

may be estimated using Eq. (2) within the thermodynamic perturbation theory by expanding into the powers of the following equation:⁶

$$\frac{\gamma_{\xi}}{\gamma} = \frac{L}{L_{\xi}} \left(\frac{\Delta \rho_{\xi}}{\Delta \rho} \right)^2. \quad (3)$$

The subscript “ ξ ” here denotes the “perturbed” functions, i.e., functions corresponding to the system with the shifted thermodynamic state. Assume that the interface thickness is proportional to the density fluctuation correlation radius in bulk liquid near the interface:⁶

$$L \sim R_{cl}, \quad R_{cl} \sim \rho_l \sqrt{K_{Tl}}, \quad (4)$$

where $K_{Tl} = \rho_l^{-1} (\partial \rho / \partial P)_{Tl}$ is the isothermal compressibility of liquid.

Our assumption is justified by the fact that for temperatures far from critical $\rho_l \gg \rho_g$ and most of the mass of the interfacial layer is concentrated in thin zone at the liquid side of the interface. In the vicinity of the critical point the values of density fluctuation correlation radii in both bulk phases are very close and our assumption is valid too. Combining Eqs. (3) and (4) we finally get:

$$\frac{\gamma_{\xi}}{\gamma} = \frac{\rho_l}{\rho_{l\xi}} \left(\frac{\Delta \rho_{\xi}}{\Delta \rho} \right)^2 \left(\frac{K_{Tl}}{K_{Tl\xi}} \right)^{1/2}. \quad (5)$$

Now if one knows the temperature difference in the interfacial layer, it is possible to use these values as the small parameters for expansion in powers of the “perturbed” functions in Eq. (5).

Consider the evaporation of a liquid layer with a plane phase boundary. Let the initial state of a system be an equilibrium state, i.e., $P_l = P_g = P_s$ and $T_l = T_g = T_s$. For slow evaporation the pressure is not changed, the vapor is saturated, and the liquid is superheated. The surface tension is determined by the temperature of the bulk liquid at the interface T_l , which in this case is equal:

$$T_l = T_s + |\nabla T| L, \quad (6)$$

where $|\nabla T| = \partial T / \partial z$ is the temperature gradient in the liquid. This temperature gradient may be estimated with the aid of the heat flux at the evaporating surface q_l :

$$T_l = T_s + \frac{q_l}{\lambda_l} L, \quad (6a)$$

where λ_l is the thermal conductivity of liquid. The difference $T_l - T_s$ is the small parameter for respective expansion of Eq. (5). For example, $\rho_{l\xi} / \rho_l \approx 1 + \rho_l^{-1} (\partial \rho_l / \partial T)_P (T_l - T_s)$, and so on. With some algebra we get the corrections for the surface tension of the evaporating system γ_{evap} in the terms of the thermodynamic properties of the coexisting phases with the plane phase boundary:

$$\frac{\gamma_{\text{evap}}}{\gamma} = 1 + \frac{L \beta_{Tl} |\nabla T|}{2} \left\{ \frac{4 \rho_l}{\Delta \rho} - 3 - C_l(T) \right\}, \quad (7)$$

where $\beta_T = \rho^{-1} (\partial \rho / \partial T)_P$ and:

$$C_l(T) = \frac{1}{\rho_l} \left[\left(\frac{\partial^2 P}{\partial V^2} \right)_T \left/ \left(\frac{\partial P}{\partial V} \right)_T \right. - \left(\frac{\partial^2 P}{\partial V \partial T} \right) \left(\frac{\partial T}{\partial P} \right)_{V,l} \right] < 0,$$

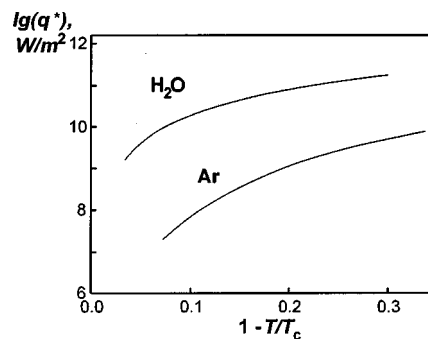


FIG. 1. Values of the characteristic heat fluxes q^* calculated for water and argon.

$C_l(T)$ should be calculated using the properties of the liquid at the coexistence line. Far from the critical point for argon $C_l(T) \approx -10$, the properties were calculated using the experimental data from the reference book;⁷ for convenience the derivatives may be estimated using one of the equations of state. For evaporation when the temperature gradient at the interface is constant, we can rewrite Eq. (8) in the following form:

$$\frac{\gamma_{\text{evap}}}{\gamma} = 1 - \frac{q_l}{q^*}, \quad (7a)$$

where

$$q^* = - \frac{2 \lambda_l}{L \beta_{Tl}} \left\{ \frac{4 \rho_l}{\Delta \rho} - 3 - C_l(T) \right\}^{-1} > 0.$$

The explicit equation for the interface thickness L may be found if we know the density profile. We used the density profile in the form of hyperbolic tangent obtained within van der Waals theory in the vicinity of the critical point.¹ According our supposition [Eq. (4)] we replaced the properties within the interfacial layer with the properties of the liquid at the phase boundary:

$$L = 24 \gamma K_{Tl} \left(\frac{\rho_l}{\Delta \rho} \right)^2. \quad (8)$$

Below we will test the correctness of this expression comparing the interface thickness calculated with the aid of Eq. (8) with the results of molecular dynamics simulation.

Obviously, this technique cannot be applied for exact calculations at high heat fluxes $q_l \approx q^*$. The characteristic heat flux q^* corresponds to conditions for which the interface became unstable because of strong decreasing of the surface tension, the values of the characteristic heat flux for argon and water are pictured in Fig. 1, calculations were performed using data from the reference book.⁷

Our calculations for argon showed that this effect on γ becomes significant when the temperature difference in the interfacial layer becomes about 1 K; that means that heat flux at the interface is about $q \sim 10^7 - 10^8$ W/m², the lower value corresponds to high temperatures $T/T_c \sim 0.9$, and the higher value to low temperatures $T/T_c \sim 0.7$. Such values of the heat flux can be reached at evaporation of liquids under the action

of the laser radiation, in experiments with wire electrical explosion, and at evaporation of microfilms of liquids on heated surfaces.

These simple equations for the surface tension corrections are based on the modified van der Waals theory of capillarity¹ and on the assumptions that lead to Eq. (5). The range of validity of this technique corresponds to temperatures higher than $(0.7-0.8)T_c$, i.e., in particular, $T > 420$ K for water and $T > 105$ K for argon, but as pointed out in Ref. 6, for simple liquids the structure of relations for the surface tension is preserved in the first approximation up to the triple point. The results of this approach will be compared with the results of molecular dynamics simulations of evaporation into vacuum below, with the aim to verify our assumptions.

III. MOLECULAR DYNAMICS SIMULATIONS

In our simulation we used a shifted Lennard-Jones potential as the intermolecular potential for the system of $N = 12\,000$ particles:

$$u(r) = \begin{cases} 4\epsilon[(\sigma/r)^{12} - (\sigma/r)^6] + u_{\text{shift}}, & \text{if } 0 < r \leq r_{\text{cut}} \\ 0, & \text{if } r_{\text{cut}} < r \end{cases},$$

$$u_{\text{shift}} = -4\epsilon[(\sigma/r_{\text{cut}})^{12} - (\sigma/r_{\text{cut}})^6], \quad (9)$$

where r is the intermolecular distance, and ϵ and σ are the potential parameters. For argon they are equal to $\epsilon/k_B = 119.8$ K and $\sigma = 0.3405$ nm. The cutoff radius for the interaction potential was set to be $r_{\text{cut}} = 3.5$ and $u_{\text{shift}}/k_B = -0.26$ K. Calculations were performed using the reduced variables; ϵ and σ were taken as units, which is commonly utilized. The MD unit of mass was set to be equal $m = 48$, that is 1.3838×10^{-27} kg for argon. For argon the unit of time is 3.114×10^{-13} s, the unit of pressure is 41.90 MPa, the unit of density is 1682.5 kg/m³, the unit of velocity is 1093.3 m/s, and the unit of surface tension is 14.26 mN/m. All the particles were placed in a rectangular MD cell with dimensions $30 \times 30 \times 60$. Periodical boundary conditions were imposed on the system in the x and y directions and an interface was formed parallel to the x - y plane. For modeling the bulk liquid, at the floor of the cell ($z = -30$), an additional potential was applied:

$$u_b(z_i) = 4\epsilon_b[(\sigma/(30+z_i))^{12} - (\sigma/(30+z_i))^6], \quad (10)$$

where z_i is the z coordinate of the particle number i . The values of ϵ_b were chosen at preparing to the simulation with the aim to provide stability of the liquid layer. For different temperatures $\epsilon_b = 0.5, \dots, 2\epsilon$. Indeed, there exists the non-physical layer (at $-30 < z < -25$) near the floor of the cell, which was not considered at the properties calculation. At $z = 30$ a repulsive potential was used:

$$u_c(z_i) = 4\epsilon_c[\sigma/(30-z_i)]^6. \quad (11)$$

In the case of evaporation into vacuum the cover of the cell was opened and $\epsilon_c = 0$; when it was closed $\epsilon_c = \epsilon$. To simulate evaporation we used a thermostat, which was an additional Langevin force acting at the floor of the MD cell:

$$\Xi_x(t) = \xi_x(t) - \beta v_x, \quad (12)$$

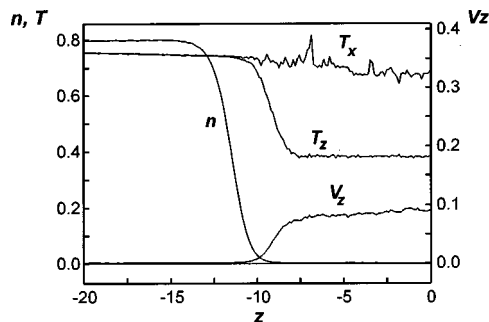


FIG. 2. Profiles of the density n , kinetic temperatures T_x , T_z and velocity V_z for evaporation into vacuum at $T_l = 0.744$.

where ξ_x is the Gaussian random force, v_x is the particle velocity, and β is the friction coefficient, other components are similar. The temperature is obtained from the thermostat parameters:⁸ $\langle \xi_x^2 \rangle = 2\beta T/h$, $h = 1/32$ is an integration time step. To integrate the equation of motion the explicit eighth-order Stoermer method was used.⁴

In order to collect data on physical properties as functions of height z , the system was divided in 512 layers $\delta z = 60/512\sigma$ parallel to the x - y plane, where the mean values were collected:

$$n(z) = \langle \delta(z_i - z) \rangle, \quad V_z(z) = \langle v_{iz} \delta(z_i - z) \rangle,$$

$$T_z(z) = 48 \langle (v_{iz} - V_z(z))^2 \delta(z_i - z) \rangle, \quad (13)$$

where v_{iz} is z -component of velocity of particle number i . Other components are similar. Obviously $V_x = V_y = 0$, T_x, T_y, T_z are the kinetic temperatures, which are equal to the thermodynamic temperature at equilibrium $T_x = T_y = T_z = T$. At nonequilibrium conditions, for example at the Knudsen layer, the kinetic temperatures can be different $T_x \neq T_y \neq T_z$.

When the equilibrium state or the stationary evaporation into vacuum were reached, an additional time averaging for about 200 000–500 000 integration time steps was used. Using the properties of equilibrium systems and data on properties of argon, we estimated the critical parameters of the MD system. The critical temperature was obtained by extrapolating the data on the surface tension to zero with the aid of experimental approximation for the surface tension of argon,⁹ also the critical temperature and density were obtained by comparing the saturation line of the MD system with the saturation line of argon.⁷ The critical temperature of the MD system $T_c = 1.21 = 145$ K is lower than the critical temperature of argon $T_c = 1.26 = 150.86$ K. The critical densities of the system and argon coincide within the simulation error: $n_c = 0.318 = 538.5$ kg/m³. The properties of the MD system and argon show good agreement in the reduced coordinates T/T_c and n/n_c .

Figures 2 and 3 show typical profiles of density, temperature, and velocity for evaporation into vacuum. The high gradients of temperature and density exist in the liquid due to high heat fluxes at evaporation. The evaporating gas is at strongly nonequilibrium conditions ($T_x \neq T_z$). The simulations were performed for the range of temperatures between 0.75 (90 K) and 1.0 (120 K). The thermodynamic properties

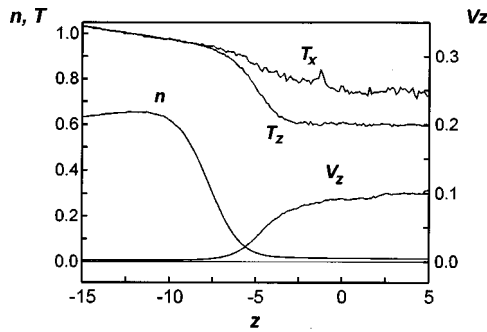


FIG. 3. Profiles of the density n , kinetic temperatures T_x , T_z and velocity V_z for evaporation into vacuum at $T_l=0.963$.

of equilibrium and nonequilibrium systems are collected in the Tables I and II. The subscript “ s ” denotes the equilibrium properties and the subscript “ i ” denotes the properties of the evaporating systems. For evaporation two values of temperature are presented: the temperature of the bulk liquid at the interface boundary T_l and the temperature of the equimolar dividing surface T_e . The values of pressure contain large errors due to computational difficulties. For the equilibrium system the virial part of pressure denoted by the superscript “ $*$ ” is presented. The procedure of the pressure calculation is described below.

IV. THE STRUCTURE OF THE INTERFACIAL LAYER

At simulations we collected data on the conditional singlet density $n_2(\mathbf{r}_1; \mathbf{r}_2)$ —the density at \mathbf{r}_2 given that there is a particle fixed at \mathbf{r}_1 . In uniform phase the conditional singlet density is a function of interparticle distance $r=|\mathbf{r}_2-\mathbf{r}_1|$, so $n_2(r)/n=g(r)$, where $g(r)$ is the radial distribution function. In a two-phase system with plane interface the density profile depends on z only [$n=n(z)$], so that the function n_2 is a function of three arguments: $n_2=n_2(z_1; z_2, r_{12})$. This function, however, cannot be found from the results of MD experiment because of computational limitations. To reduce the numerical work we set $z_1=z_2$. Thus we consider the density correlations in the x - y plane at different $z=z_1=z_2$. If, for a given pair of particles $i-j$ the z -coordinates belong to the same thin layer, we include this pair in the calculation of n_2 . The interval of interparticle distances $0.5 < r_{ij} < 15$ was divided into 512 layers. We defined the density fluctuation correlation length through the moments of the correlation function.

Consider the density–density correlation function in a uniform phase with the density $n(\mathbf{r})$:

$$\langle n(\mathbf{R})n(\mathbf{R}+\mathbf{r}) \rangle = n\delta(\mathbf{R}) + n^2 g(|\mathbf{r}|). \quad (14)$$

The density fluctuation correlation function may be derived from Eq. (14) as:

$$\begin{aligned} h(r) &\equiv \langle [n(\mathbf{R}) - n][n(\mathbf{R}+\mathbf{r}) - n] \rangle \\ &= n\delta(\mathbf{R}) + n^2(g(|\mathbf{r}|) - 1). \end{aligned} \quad (15)$$

Let us define the correlation length R_c as:

$$R_c = \frac{\int r h(r) d\mathbf{r}}{\int h(r) d\mathbf{r}}, \quad (16)$$

where interparticle distance is equal $r=|\mathbf{r}|$. Substituting $h(r)$ into Eq. (16) yields the following formula for the correlation length:

$$R_c = \frac{4\pi n \int_0^\infty (g(r) - 1)r^3 dr}{1 + 4\pi n \int_0^\infty (g(r) - 1)r^2 dr}. \quad (17)$$

This relation is obtained for a homogeneous phase, but we use it to investigate correlations inside the interfacial layer using the correlation function calculated in the x - y plane. There exists the high level of error for R_c in bulk liquid due to the low compressibility of liquid.

The correlation lengths for all temperatures are found to be equal for different positions z inside the interfacial layer and R_c at the interface is greater than the correlation length in the bulk phases. This surprising result may be explained by the fact that the correlation length at the interface is limited by the size of the MD cell. In order to test this supposition we have made additional simulation of two equilibrium systems at $T=0.8$ with $r_{\text{cut}}=2.5$. The first contained 12 000 particles with interface area 30×30 and the second contained 108 000 particles with interface area 90×90 . Other conditions were identical. Profiles of density and temperature for the system of 12 000 are shown at Fig. 4. Characteristic profiles of n_2 for this system are pictured on Figs. 5 and 6. Calculations showed that on the way from liquid to gas the high-order coordination spheres disappear first, and the positions of maxima do not change. Also the long-range fluctuations of density are found inside the transition layer—the long “tails” of the distribution functions. The results of R_c calculation are shown in Fig. 7. One can see that the correlation length for the big system is three times greater than the correlation length for small system; likewise the size of the cells.

Based on the results of the MD simulations we may draw the following conclusions. The interface is the strong correlated area and the correlation length along the interface is limited only by the size of the system. There exists the

TABLE I. Parameters of the equilibrium liquid–gas systems.

T_s	0.752	0.801	0.842	0.900	0.952	1.000
n_{ls}	0.800	0.777	0.753	0.725	0.696	0.665
n_{gs}	0.0061	0.0096	0.0146	0.0218	0.0285	0.0432
P_{ls}^*	−0.597	−0.614	−0.627	−0.636	−0.638	−0.631
$P_{gs}^*, 10^{-3}$	−0.23	−0.53	−1.2	−2.5	−4.7	−8.9
$P_s, 10^{-3}$	4.35	7.16	11.2	17.1	23.6	34.3
L	2.02	2.24	2.43	2.66	3.03	3.52

TABLE II. Parameters of the liquid–gas systems at evaporation into vacuum.

T_{li}	0.744	0.795	0.841	0.891	0.927	0.963
T_{ei}	0.743	0.793	0.836	0.882	0.912	0.940
$(\partial T/\partial z)_{li}, 10^{-3}$	-1.59	-2.33	-4.02	-6.12	-9.42	-12.84
n_{li}	0.803	0.780	0.756	0.731	0.710	0.692
$(\partial n/\partial z)_{li}, 10^{-3}$	0.76	1.26	2.13	3.89	6.69	11.05
$P_{il}, 10^{-3}$	1.9	4.0	11.	13.	14.	25.
L_i	1.97	2.27	2.52	2.88	3.18	3.58

tendency to preserve short-range order in the interfacial layer, which is why, the local density (which can be determined on the scale $2-3\sigma$) has only two values—the liquid density and the gas one. The amplitudes of density fluctuations (“capillary waves”) inside the interfacial layer determine the monotonous average density profile and the interface thickness L , which increases with the temperature. This fact is in good agreement with the van der Waals capillarity theory as well as with the capillary-wave theory.¹

V. THE SURFACE TENSION

The surface tension was calculated by a commonly used method with the use of the pressure tensor:¹

$$\gamma = \int_{z_l}^{z_g} (P_z(z) - P_x(z)) dz, \quad (18)$$

where $P_z = P_{zz}$ and $P_x = (P_{xx} + P_{yy})/2$ are the pressure components normal and tangential to the surface. In the bulk phases $P_z = P_x = P$, where P is the thermodynamic pressure, the following general relation for the pressure¹⁰ was used:

$$\begin{aligned} \hat{P}_{xy}(\mathbf{r}) = & \sum_i m v_{xi} v_{yi} \delta(\mathbf{r} - \mathbf{r}_i) \\ & - \frac{1}{2} \sum_{i \neq j} \frac{x_{ij} y_{ij}}{r_{ij}} \frac{\partial u(r_{ij})}{\partial r_{ij}} \int_0^1 d\eta \delta(\mathbf{r} - \mathbf{r}_i + \eta \mathbf{r}_{ij}). \end{aligned} \quad (19)$$

Other components are similar. Averaging over time and taking into account the periodic boundary condition one can obtain P_z and P_x :

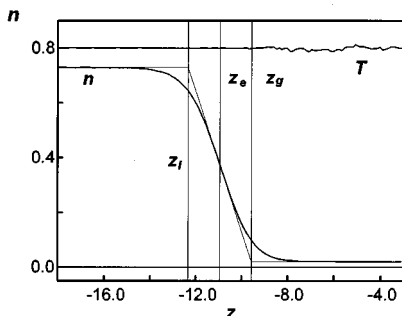


FIG. 4. Profiles of the density n and temperature T for equilibrium system of 12 000 particles with $r_{cut}=2.5$, $T_s=0.80$, liquid boundary $z_l=-12.4$, $n=0.730$, equimolar dividing surface $z_e=-11.0$, $n=0.375$, gas boundary $z_g=-9.6$, $n=0.020$.

$$\begin{aligned} P_z(z) &= n(z)T_z(z) + P_z^*(z), \quad P_x(z) = n(z)T_x(z) + P_x^*(z), \\ P_z^*(z) &= -\frac{1}{2L^2} \left\langle \sum_{i \neq j} \frac{z_{ij}^2}{r_{ij}} u'(r_{ij}) \mathcal{D}(\mathbf{r}, \mathbf{r}_i, \mathbf{r}_j) \right\rangle, \\ P_x^*(z) &= -\frac{1}{2L^2} \left\langle \sum_{i \neq j} \frac{(x_{ij}^2 + y_{ij}^2)}{2r_{ij}} u'(r_{ij}) \mathcal{D}(\mathbf{r}, \mathbf{r}_i, \mathbf{r}_j) \right\rangle, \\ \mathcal{D}(\mathbf{r}, \mathbf{r}_i, \mathbf{r}_j) &\equiv \int_0^1 d\eta \delta(\mathbf{r} - \mathbf{r}_i + \eta \mathbf{r}_{ij}). \end{aligned} \quad (20)$$

The main difficulty is in the additional integration over the parameter. The virial contribution into the pressure tensor P^* is commonly shared into equal parts between points r_i and r_j , which means that the integral in Eq. (20) is estimated by the trapezoid rule:

$$\mathcal{D}(\mathbf{r}, \mathbf{r}_i, \mathbf{r}_j) \approx (\delta(\mathbf{r} - \mathbf{r}_i) + \delta(\mathbf{r} - \mathbf{r}_j))/2. \quad (21a)$$

Our MD simulation has shown that in this case the mechanical equilibrium condition is broken within the layer where the density gradient is high ($P_z \neq \text{Const}$; see Fig. 8). To improve the pressure calculation quality we propose to use the Simpson rule for the integral in Eq. (20):

$$\mathcal{D}(\mathbf{r}, \mathbf{r}_i, \mathbf{r}_j) \approx [\delta(\mathbf{r} - \mathbf{r}_i) + 4\delta(\mathbf{r} - (\mathbf{r}_i + \mathbf{r}_j)/2) + \delta(\mathbf{r} - \mathbf{r}_j)]/6. \quad (21b)$$

Figure 9 shows that by using of Eq. (21b) a better accuracy is reached than with the use of Eq. (21a). Note that the way of integrating Eq. (20) has no influence on the value of the surface tension.

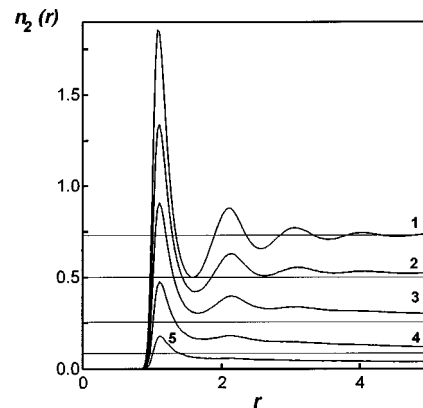


FIG. 5. The conditional singlet density n_2 in the interfacial layer for equilibrium system at $T_s=0.8$, which is shown at Fig. 4. The thin lines show the values $n(z)$, which are the limit values for $n_2(r)$: (1) $-z=-19$, $n=0.730$ (bulk liquid); (2) $z=-11.5$, $n=0.494$; (3) $z=-10.5$, $n=0.253$; (4) $z=-9.5$, $n=0.085$; (5) $z=-8.5$, $n=0.032$.

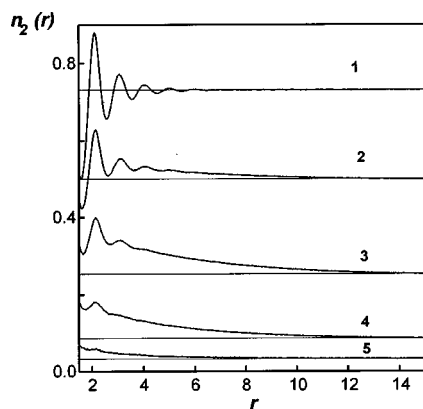


FIG. 6. The “long tails” of the distribution function. The conditional singlet density n_2 in the interfacial layer for equilibrium system at $T_s=0.8$, which is shown in Fig. 4. See caption for Fig. 5.

For the nonequilibrium process of evaporation a kinetic term appears in the surface tension:

$$\gamma_k = \int_{z_l}^{z_g} n(z)(T_z(z) - T_x(z))dz. \quad (22)$$

Calculations show that this term is not negligible for the intense evaporation. The results of the molecular dynamics simulations are gathered in Table III. For the equilibrium state the kinetic term $\gamma_{sk} \equiv 0$ and nonzero values of γ_{sk} obtained in the simulation represent the error level for the values of surface tension.

VI. THE EVAPORATION COEFFICIENT

The evaporation coefficient α represents the probability for a molecule to escape from the liquid surface. For the evaporation into vacuum α is the ratio of the real flux of evaporated particles j to the maximum flux density of atoms evaporated from the surface of a condensed body j_{\max} , which is given by the Hertz formula:

$$j_{\max} = n_s \left(\frac{k_B T}{2\pi m} \right)^{1/2} = n_s \left(\frac{T}{96\pi} \right)^{1/2}, \quad (23)$$

where n_s is the density of equilibrium vapor at T . We used this macroscopic definition of the evaporation coefficient and found that its value is strongly influenced by the choice of the reference surface temperature. We used two tempera-

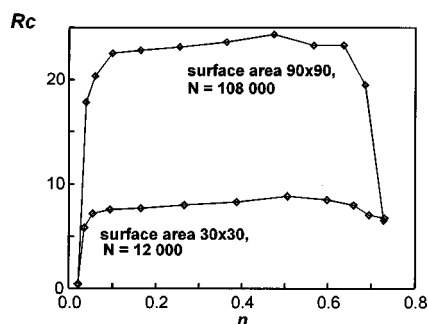


FIG. 7. The density fluctuations correlation lengths calculated across the interface of equilibrium systems with different surface areas A and numbers of particles N at temperature $T_s=0.8$.

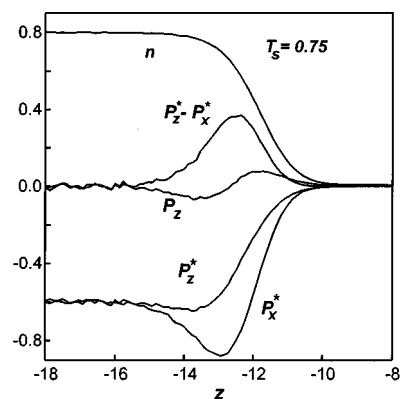


FIG. 8. The pressure tensor of the equilibrium system $T_s=0.75$ calculated by Eq. (20a). One can see that mechanical equilibrium is broken in the interfacial layer ($P_z \neq \text{Const}$).

tures; the first was the temperature of the bulk liquid at the interface T_l and the second was the temperature of the dividing surface where the evaporation begins T_{Kn} , i.e., the velocity V_z becomes nonzero and appears the difference between the kinetic temperatures T_x and T_z (see Figs. 3 and 4). Obviously the position of the dividing surface corresponding to T_{Kn} cannot be determined better than δz and the evaporation coefficient error level is about ± 0.1 . In the first case the evaporation coefficient is found to be a function of the mass flux j . In contrast, for T_{Kn} the evaporation coefficient is practically independent of the mass (or heat) flux and has the value equal to $\alpha \approx 0.8$ (see Table IV). The last result is in a good agreement with the theoretical predictions¹¹ and the recent computer simulations⁵ in which another microscopic algorithm for α calculation was used.

VII. DISCUSSION

As was said above, our purpose here was to compare thermodynamic approach results with those for model Lennard-Jones system. We have made our main assumption at thermodynamic analysis when we supposed that the interface thickness is proportional to the density correlation fluctuation radius in the bulk liquid near the phase boundary. We calculated the interface thickness during the MD simulations

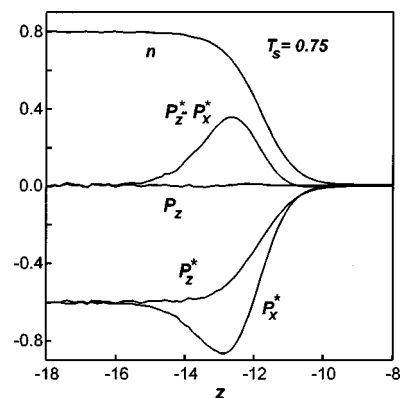


FIG. 9. The pressure tensor of the equilibrium system $T_s=0.75$ calculated by Eq. (20b). The mechanical equilibrium is proved in the interfacial layer ($P_z = \text{Const}$).

TABLE III. The surface tension.

T_s	Equilibrium systems					
	0.752	0.801	0.842	0.900	0.952	1.000
γ_s^*	0.759	0.664	0.583	0.472	0.376	0.291
γ_{sk}	0.0016	0.0019	0.0025	0.0026	-0.0001	0.0014
γ_s	0.760	0.666	0.585	0.475	0.376	0.292
T_{li}	Evaporation into vacuum					
	0.744	0.795	0.841	0.891	0.927	0.963
T_{ei}	0.743	0.793	0.836	0.882	0.912	0.940
γ_i^*	0.768	0.673	0.584	0.488	0.419	0.350
$\gamma_{ik}(T_{li})$	-0.0068	-0.0079	-0.0081	-0.0119	-0.0194	-0.0212
$\gamma_i(T_{li})$	0.761	0.665	0.576	0.477	0.399	0.329

using Eq. (1); in our calculations the coordinate z cannot be calculated better than the size of z -slab: $\delta z = 60/512 = 0.117$, so the error for L is about 5%–10%. These values were compared with the interface thickness calculated for argon using Eq. (5) (see Fig. 10) with an agreement within the simulation error. One can see that evaporation causes an increase of the interface thickness that results in modification of the surface tension. Thus the validity of this assumption is proved. Also the parameter $m[\rho]$ from Eq. (4) was calculated from the MD results and proved to be constant.

Because of the presence of the temperature gradient at the interface and the finite size of the interfacial layer, the problem of reference temperature for the surface tension appears. Thermodynamic analysis shows that γ is determined by the state of the bulk liquid near the interface, which has the temperature that differs from the temperature of any dividing surface usually used (e.g., surface of tension or equimolar dividing surface). That is why the correction for the surface tension of evaporating system appears. The values of the surface tension of the evaporating systems γ_i obtained in the MD simulation were compared with the surface tension of equilibrium MD systems γ_s . We use two reference temperatures for γ_i . The first is the temperature of the bulk liquid near the interface T_l ; this temperature corresponds to the maximum density (see Figs. 2 and 3). The second one is the temperature of the equimolar dividing surface (the Gibbsian zero-adsorption dividing surface) $T_e < T_l$. In the first case the values of surface tension for the equilibrium and nonequilibrium systems were found to be roughly equal $\gamma_i \approx \gamma_s(T_l)$. For the second case, obviously, $\gamma_i < \gamma_s(T_e)$. The difference $(\gamma_i - \gamma_s(T_e))/\gamma_s(T_e)$ was compared with the surface tension correction obtained within the thermodynamic approach [Eqs. (8) and (8a)]. The characteristic heat flux q^* was calculated using the data on the prop-

TABLE IV. The evaporation coefficient.

$j, 10^{-3}$	0.228	0.369	0.584	0.836	1.150	1.468
T_{li}	0.744	0.795	0.841	0.891	0.927	0.963
$\alpha(T_l)$	0.752	0.747	0.753	0.703	0.667	0.590
T_{Kn}	0.743	0.793	0.838	0.888	0.920	0.953
$\alpha(T_{Kn})$	0.85	0.78	0.83	0.80	0.84	0.82

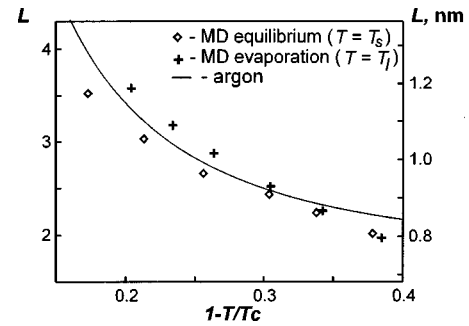


FIG. 10. The interface thickness. Comparison of MD calculations from the density profiles by Eq. (1) (dots) with calculations by Eq. (8) using argon properties (Ref. 7) (solid line).

erties of argon⁷ at the same reduced temperature as T_e/T_c . The heat flux q_l was calculated using the real temperature gradient from the evaporation simulation. The results are presented in Fig. 11. Although the error level for surface tension calculation is not less than 10% we got the quantitative agreement between the results of MD simulation and thermodynamic approach. Thus it is possible to calculate the correction to the surface tension of the nonequilibrium system using the properties of the equilibrium bulk phases with the aid of the simple thermodynamic approach [Eqs. (7) and (7a)].

The evaporation coefficients were calculated using the results of the MD simulation and Eq. (23) as definition. It was shown that different choices of the reference temperatures for the evaporation coefficient lead to different behavior of α . The temperature of the bulk liquid T_l being chosen as the reference temperature leads to temperature dependence of the evaporation coefficient $\alpha = \alpha(T)$, with increasing as the temperature α decreases. In contrast, the choice of T_{Kn} as the reference temperature makes α independent of the temperature. This fact may explain the difficulties of the experiments on the evaporation coefficient and disagreements in the experimental results.

In conclusion note that all of these examples show the necessity of entering the various phase boundary tempera-

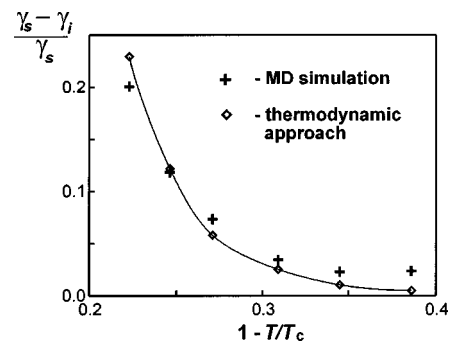


FIG. 11. Comparison of the surface tension correction obtained within thermodynamic approach and calculated by Eq. (7) using the properties of argon (Ref. 7) and the temperature gradients obtained at MD simulation with the surface tension correction calculated using the values of the surface tension of equilibrium system $\gamma_s(T_e)$ and evaporating system γ_i . The solid line is plotted to guide the eye.

tures for solving different heat mass transfer problems under highly nonequilibrium conditions.

This study was supported by the Russian Foundation for Basic Research; Projects No. 96-02-17546, No. 98-02-16855. One of the authors (V.V.Z.) gratefully acknowledges the support of his work by the Japan Society for the Promotion of Science (ID No. PG8042).

¹J. S. Rowlinson and B. Widom, *Molecular Theory of Capillarity* (Clarendon, Oxford, 1982).

²I. Tanasawa, *Heat Transfer 94. Proceedings of the 10th International Heat Transfer Conference, Brighton, U.K.*, edited by G. F. Hewitt (Inst. of Chemical Engineering, 1994), Vol. 1, p. 297.

³D. A. Labuntzov and A. P. Kryukov, *Int. J. Heat Mass Transf.* **20**, 989–1002 (1979).

⁴V. V. Zhakhovskii and S. I. Anisimov, *JETP* **84**, 734 (1997).

⁵K. Ysuoka, M. Matsumoto, and Y. Kataoka, *J. Chem. Phys.* **101**, 7904 (1994).

⁶S. P. Malysenko, *High Temp.* **32**, 671 (1994).

⁷N. B. Vargaftik, *The Reference Book about Thermophysical Properties of Gases and Liquids* (Nauka, Moscow, 1972) (in Russian).

⁸D. W. Heerman, *Computer Simulation Methods in Theoretical Physics* (Springer Verlag, Berlin, 1986).

⁹V. G. Baidakov, *The Interface of the Simple Classical and Quantum Liquids* (Nauka, Ekaterinburg, 1994) (in Russian).

¹⁰F. M. Kuni, *Statistical Physics and Thermodynamics* (Nauka, Moscow, 1981) (in Russian).

¹¹S. I. Anisimov, ed., *Physical Kinetics and Transport Processes of Phase Transitions* (Nauka i Tekhnika, Minsk, 1980) (in Russian).